



## Research Article

**Influences of post-weld artificial aging on microstructural and tensile properties of friction stir-welded Al-Zn-Mg-Si-Cu aluminum alloy joints**Dilek ARSLAN<sup>a</sup> and Safiye İPEK AYVAZ<sup>b,\*</sup> <sup>a</sup> *Izmir Democracy University, Faculty of Engineering, 35140, Izmir, TÜRKİYE.*<sup>b</sup> *Manisa Celal Bayar University, Turgutlu Vocational School, 45400 Manisa, TÜRKİYE.*

## ARTICLE INFO

## ABSTRACT

## Article history:

Received 15 May 2024

Accepted 07 August 2024

Published 20 August 2024

## Keywords:

Aluminum alloy

Friction stir welding

Microstructure

Mechanical properties

Post weld heat treatment

In this study, the effect of heat treatment on the mechanical and microstructural properties of welded joints after friction stir welding of age-hardenable Al-Zn-Mg-Si-Cu wrought aluminum alloy plates was investigated. For this purpose, some of the samples welded using FSW technique with a rotational speed of 1250 rpm and a traverse speed of 40 mm·min<sup>-1</sup> were subjected to annealing and some to artificial aging heat treatment at different temperatures and times. In FSWed artificial aged samples where AlFeSi precipitate formations were detected, hardness and strength increase were realized with grain-boundary strengthening and Orowan hardening mechanisms. The lowest ultimate tensile strength was 156.3 N·mm<sup>-2</sup> in the annealed sample, while the highest ultimate tensile strength was 210.8 N·mm<sup>-2</sup> in the sample artificially aged at 190 °C for 2 hours. Fractographic examination revealed that ductile fracture occurred in all specimens.

**1. Introduction**

Aluminum and its alloys, with their low specific gravity, high strength and improved corrosion resistance, are now widely used in areas requiring high mobility, such as automotive, aerospace and defense [1–7]. Similar and dissimilar welded aluminum joints and its alloys are needed in these areas. However, the weldability of the most widely used age-hardenable Al-Cu, Al-Cu-Mg and Al-Zn-Mg-Cu alloys is poor with fusion welding methods such as gas tungsten arc welding [8–11]. This is because during the re-solidification of the molten zone after welding, defects such as microstructural changes and solidification cracking occur, which negatively affect the mechanical properties [12]. In addition, lower distortions and residual stresses occur with lower heat input [13]. For this purpose, solid-state welding methods are used for age-hardenable 2XXX and 7XXX series aluminum alloys. Friction stir welding (FSW) is one of the solid-state welding methods used for welding aluminum and its alloys [10]. The Weld Institute of Cambridge in the UK developed and patented this technique in 1991 [12,14]. In the FSW technique, two plates to be joined are joined by dynamically stirring the two parts together using a tool that rotates on the joint surface [15]. In addition to preventing solidification cracking with this method without melting,

significant grain refinement occurs due to dynamic recrystallization in the nugget zone [11,12].

Artificial aging increases the strength of aluminum alloys and welded joints. If heat treatment is applied before welding, the precipitates in fusion welds may dissolve again due to the high temperature. In FSW, although the melting temperature is not reached, microstructural distortions may occur due to high temperature and high plastic deformation in the weld zone [16]. In addition, many studies have reported that intermetallic precipitates are re-dissolved by the FSW process after aging [17–19]. For this reason, the post-welding heat treatment (PWHT) of FSWed aluminum alloys is a strength enhancement method. In the literature, there are several studies investigating the effect of post-welding heat treatment on the mechanical properties of aluminum alloys such as AA2014 [20], AA2024 [21], AA 6061 [22,23], AA7039 [24], AA7075 [13] etc., joined by friction stir welding. Most of the studies in the literature have focused on post-weld heat treatment [25–28]. This is because friction stir welding of peak-aged aluminum alloy reduces tool life due to higher resistance to deformation [29].

Yadav et al. subjected AA2024 aluminum alloy to an artificial aging process after FSW. It was reported that the yield and tensile strengths, as well as the ductility of the

\* Corresponding author. Tel.: +90-236-234-44 61; Fax: +90-236 -201-29 97.

E-mail addresses: [safiye.ipek@cbu.edu.tr](mailto:safiye.ipek@cbu.edu.tr) (S. İpek Ayvaz), [da.dilekarslan@gmail.com](mailto:da.dilekarslan@gmail.com) (D. Arslan)

ORCID: 0000-0001-7385-7388 (S. İpek Ayvaz), 0000-0003-0198-0787 (D. Arslan)

DOI: [10.35860/iarej.1484578](https://doi.org/10.35860/iarej.1484578)© 2024, The Author(s). This article is licensed under the [CC BY-NC 4.0](https://creativecommons.org/licenses/by-nc/4.0/) International License (<https://creativecommons.org/licenses/by-nc/4.0/>).

specimens, increased with PWHT [21]. When Feng et al. applied PWHT to FSWed AA2219-O, it was reported that the strength of the welded joint increased, although grain coarsening occurred in the stir zone (SZ) [30]. Sabari et al. performed tests with untreated AA2519, welded, artificially aged, solution treated and artificially aged FSWed AA2519 specimens and obtained the best mechanical properties in the solution-treated and artificially aged FSWed AA2519 specimen [31]. Pabandi et al. investigated the effects of precipitation hardening solution treatment and artificial aging heat treatment on the mechanical and microstructural properties of FSWed AA6061-T6-AA2024-T6. They found that PWHT increased the weld strength [32]. Sharma et al. reported that the mechanical properties of FSWed Al-Zn-Mg aluminum alloy specimens increased with natural aging, while only the solution-treated specimens showed a decrease in mechanical properties [24]. As seen in many studies in the literature, the increased tensile strength will be achieved by obtaining a precipitated and fine-grained microstructure with a homogeneous distribution in the weld zone.[33]. Most of the studies in the literature have focused on post-weld heat treatment. This is because friction stir welding of peak-aged aluminum alloy reduces tool life due to higher resistance to deformation.

This study selected the Al-Zn-Mg-Si-Cu alloy, widely used in the automotive, aerospace and defence industries but not recommended for fusion welding. The effects of annealing and artificial aging on this alloy's microstructural and mechanical properties after friction stir welding were investigated.

## 2. Materials and Methods

In this study, wrought aluminum alloy with dimensions of 500x80x5 mm sheets were used. The chemical composition of the aluminum alloy used is presented in Table 1. The samples were welded using the friction stir welding (FSW) machine (Beijing FSW Technology Co.) with an FSW-LM-BM 16-2D Gantry Model. The FSW process was performed using a rotational speed and a traverse speed of 1250 rpm and 40 mm·min<sup>-1</sup>, respectively. The images of the 4 mm long pin and shoulder made of H13 tool steel used are given in Figure 1. After the FSW process, 1 mm chips were removed from the surfaces of the joints by milling. To determine the mechanical properties of the heat treatment after FSW, some welded specimens (T0) were annealed at 415 °C for 3 hours. The remaining specimens were subjected to artificial aging heat treatment at 450 °C for 2 hours after solution and quench cooling. These specimens were coded as aging temperature-duration (190 °C-2 h, 190 °C-4 h, 205 °C-2 h, 205 °C-4 h).

The samples to be used for microstructural and mechanical investigations were removed from the welded plate by electrical discharge machining. The samples for

microstructural investigations were sanded with 100-1200 grit SiC abrasive papers in a Metkon Forcipol 1V polishing machine and then polished using 3 and 1 μ diamond solution, respectively. After polishing, the sample surfaces were etched using Keller's Reagent (1.0 mL HF, 1.5 mL HCl, 2.5 mL HNO<sub>3</sub> and 95 mL water). After the etching process, the microstructures of the samples were examined with a Nikon Eclipse LV150N optical microscope (OM) and Clemex image analysis system. Grain sizes were measured at 1000x magnification with 10 measurements from different regions and averaged. Microhardness measurements were conducted with a load and dwell time of 100 gf and 10 s, respectively, 1 mm below the surface. The measurements were conducted using the Future-Tech FM-700 Vickers micro-hardness tester (Future-Tech Corp., JAPAN). The tensile tests were carried out according to ASTM-E8-04 standard using the Shimadzu Autograph AG-IS 100kN universal testing machine. The tests were repeated five times for each specimen at room temperature with a 1 mm·sec<sup>-1</sup> strain rate. Fracture surface examinations were performed using a ZEISS GeminiSEM 500 scanning electron microscope (SEM) with a secondary electron (SE) detector from ZEISS, Oberkochen, Germany.

Table 1. Chemical composition of the aluminum alloy (wt.%)

Elements	Amount (wt. %)
Al	93.700
Zn	2.335
Si	0.912
Mg	1.022
Cu	0.912
Fe	0.485
Mn	0.196
Cr	0.129
Other	0.309



Figure 1. Photograph of FSW tool with threaded conical pin

### 3. Results and Discussion

Figure 2 shows the cross-sectional macrostructure of the samples annealed, aged at 190 °C for 2 and 4 hours and at 205 °C for 2 and 4 hours, respectively. The cross-sectional image clearly shows the different regions in the welded specimens. These regions are thermally and mechanically affected base metal (BM) at the edges, friction stir zone (FSZ) in the middle, shoulder deformation zone (SDZ) at the top and thermo-mechanically affected zone (TMAZ) between BM and FSZ. In addition, the retreating side (RS) and the advancing side (AS) were seen in the SDZ of all joints. It was found that the TMAZ was wider in RS in all samples. In addition, the heat-affected zone (HAZ) was also relatively wider in RS due to the higher temperature. Voids may form in the AS, especially when material transfer, plastic flow and temperature are insufficient [34,35]. However, as shown in Figure 2, no void, tunnel or cracking-like weld defects were detected in any region of the specimens. Onion ring-like flow bands, also detected in different studies [35–37], were observed in the FSZ region. While some of the studies explained the "onion ring" shaped band formations with the temperature differences occurring during the FSW process [38,39], some studies have found that there is a difference in precipitate and hard particle density between these bright and dark bands [40,41]. In addition, it has been reported that band formation is evident in artificially aged specimens before welding, while it loses its visibility in annealed specimens [35]. In this study, the band formation was not visible in the T0 sample due to the dissolution of precipitates during annealing after the friction stir welding (FSW) process (Fig. 2a).

In Figure 3, micrographs of the specimens taken from the FSW region are given respectively. Different microstructures in different regions of the welded joint can be detected in these micrographs. In addition to FSZ and TMAZ, HAZ can be seen at the bottom right of the micrographs. The TMAZ and HAZ are relatively narrow in these pictures taken from the AS area. In all samples, apparent grain growth was detected in the HAZ, while in the TMAZ, generally small and oriented grains were observed. Smaller but almost coaxial grains were observed in the FSZ. The average size of the FSZ grains was 3-5  $\mu\text{m}$ . Similarly, Sajadifar et al. reported the average grain size in the nugget zone of AA 7075 alloy specimens aged after welding as 2  $\mu\text{m}$  [42]. In addition, changes occurred in the microstructure of FSZ with artificial aging. Some increase in the size of  $\alpha$  aluminum grains in the FSZ of artificially aged samples was detected.

The hardness changes of FSWed specimens at the weld line after heat treatment are given in Figure 4. Post-weld heat treatment improved the microhardness of all areas.

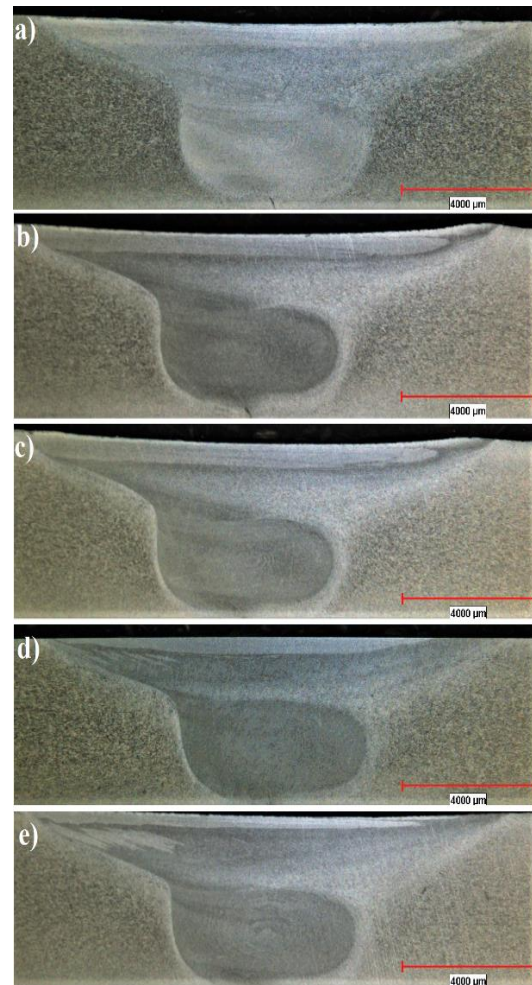


Figure 2. Cross-sectional macrostructure images of the samples: a) T0, b) 190 °C-2 h, c) 190 °C-4 h, d) 205 °C-2 h and e) 205 °C-4 h.

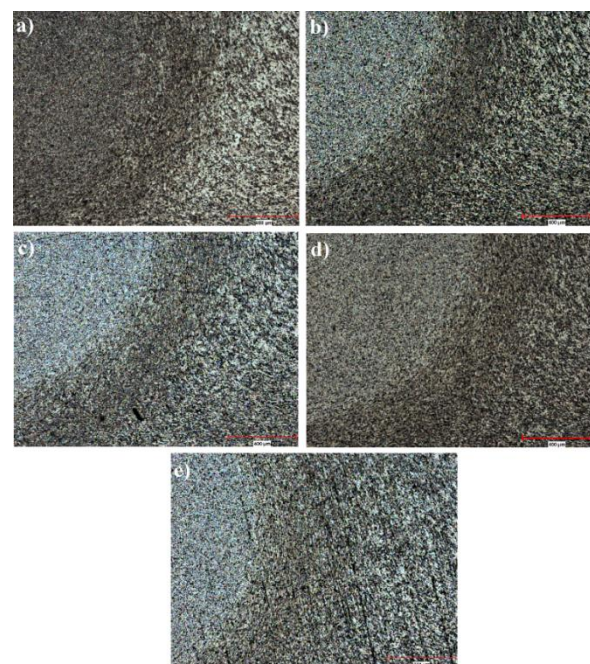


Figure 3. Cross-sectional micrographs of the samples: a) T0, b) 190 °C-2 h, c) 190 °C-4 h, d) 205 °C-2 h and e) 205 °C-4 h.

Hardness increases, especially in the HAZ, where dramatic hardness increases were observed after the welding process, were also seen in previous studies where heat treatment was performed [43]. It can be seen that the highest hardness values in all specimens are in the FSZ, and the hardness decreases from the weld center to the BM. Many studies have reported that in aluminum alloys, the combination of high plastic deformation and frictional heating effect during FSW, always in the FSZ, results in a recrystallized microstructure [1,44–48]. As is well known, grain size affects the strength of metals. The relationship between grain size ( $d$ ) and yield stress ( $\sigma_y$ ) is described by the Hall-Petch equation [48]:

$$\sigma_y = \sigma_0 + k_y d^{-1/2} \quad (1)$$

Here,  $\sigma_0$  is the friction stress, and  $k_y$  is the material constant. As can be seen from this equation, the yield strength of metallic material decreases as the grain size increases. This equation takes the following form using the  $H_v \cong 3\sigma_y$  equation between the material hardness  $H_v$  and  $\sigma_y$ :

$$H_v = H_0 + k_H d^{-1/2} \quad (2)$$

As can be seen, a decrease in grain size increases the hardness of the metallic material. For this reason, a hardness decrease from FSZ to BM was observed in all samples. Microstructural investigations revealed a slight increase in grain size in the FSZ of the artificially aged specimens compared to the annealed specimen (Figure 3). The effective mechanism for the hardness increases along the weld line in all aged specimens is precipitation hardening. The hard intermetallic precipitates formed due to artificial aging provide Orowan hardening by preventing dislocation movements. Figure 5 shows the elemental microanalysis results obtained by SEM-EDS for the 190 °C-4 h sample. The region given as Spectrum 2 is  $\alpha$  aluminum. It can be seen that the bright precipitate given as Spectrum 1 is rich in Fe, Si, and Cu. The presence of AlFeSi intermetallic precipitate has been reported in similar studies [49,50].

The influence of post-weld heat treatment on the aluminum alloy samples' ultimate tensile strength and maximum strain are summarized in Figure 6. The improvement in mechanical properties by heat treatments has also been reported in previous studies [51–53]. In an earlier study, the tensile strength of a naturally aged sample with the same chemical composition was reported as  $238.25 \text{ N}\cdot\text{mm}^{-2}$  and the elongation to fracture as 6.67% after FSW treatment with the same parameters [1]. In this study, the tensile strength of the aluminum alloy plate decreased to  $156.3 \text{ N}\cdot\text{mm}^{-2}$  and the elongation at break

decreased to 4.90% with the annealing process performed after the FSW process. For the artificially aged specimens, the highest elongation at break was 6.15 % for the specimen aged for 2 h at 190 °C. The lowest elongation at break was 3.19% for the specimen artificially aged at the same temperature for 4 h.

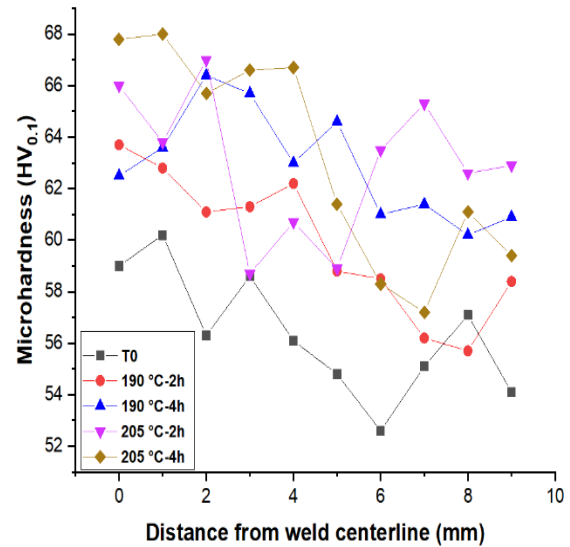


Figure 4. Variation of microhardness of the post-weld heat treated FSWed samples.

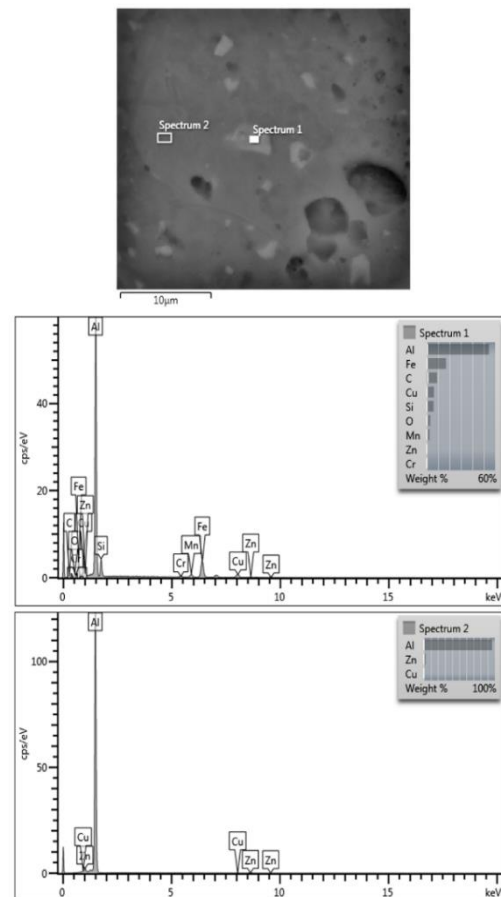


Figure 5. EDAX results for 190 °C-4 h sample.

This specimen had the highest tensile strength, and its ultimate tensile strength was  $210.8 \text{ N}\cdot\text{mm}^{-2}$ . Therefore, artificial aging at  $190 \text{ }^\circ\text{C}$  for 4 h improved the tensile strength by  $\sim 34.8\%$  compared to the annealed specimen. İpekoğlu and Çam also found that the mechanical properties of the specimens improved after heat treatment, but the ductility decreased [54]. After artificial aging at  $205 \text{ }^\circ\text{C}$  for 2 and 4 h, the mechanical properties of the specimens relatively decreased and tensile strengths of  $187.3$  and  $189.9 \text{ N}\cdot\text{mm}^{-2}$  were measured after 2 and 4 h aging, respectively. Tensile test data and  $190 \text{ }^\circ\text{C}$  and 4 h were determined as peak aging parameters for the artificial aging process of this aluminum alloy. Figure 7 shows the fractographs of annealed and artificially aged specimens after the tensile test. For all heat treatment parameters after welding, populated dimples of uniform size were observed on the fracture surfaces of all specimens, elongated in the load direction. However, it can be seen in Figure 7a that the size of the dimples decreased with artificial aging, with the largest dimples formed on the fracture surface of the annealed specimen. Course dimples and low hardness are essential indicators of low tensile strength [50]. In addition, microvoids were also observed in the course dimples in the annealed sample, where crack formation started. The size of the dimples decreased with artificial aging. Specimens artificially aged at  $190$  and  $205 \text{ }^\circ\text{C}$  for 2 h have larger dimple sizes than those artificially aged for 4 h

h at the same temperatures. In the  $190 \text{ }^\circ\text{C}$ -4 h (Fig. 7c) specimen, in addition to fine dimples, flat surfaces were observed, while less flat surfaces were detected in the  $205 \text{ }^\circ\text{C}$ -2 h (Fig. 7d) and  $205 \text{ }^\circ\text{C}$ -4 h (Fig. 7e) specimens. Fine dimples are a characteristic indicator of ductile fracture. Therefore, this specimen is the joint with the highest ductility. Fine-size dimples are also indicative of high-strength [56]. In addition to dimple formation, several tear ridges were observed on the fracture surfaces of  $190 \text{ }^\circ\text{C}$ -4 h (Fig. 7c),  $205 \text{ }^\circ\text{C}$ -2 h (Fig. 7d) and  $205 \text{ }^\circ\text{C}$ -4 h (Fig. 7e) specimens.

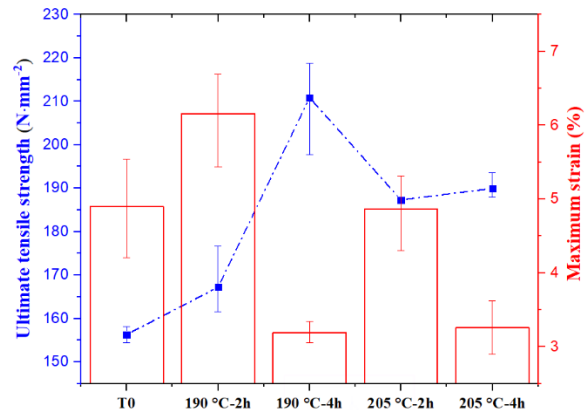


Figure 6. The effect of the of post-weld heat treatment on ultimate tensile strength and total elongation of FSWed aluminum alloy plates.

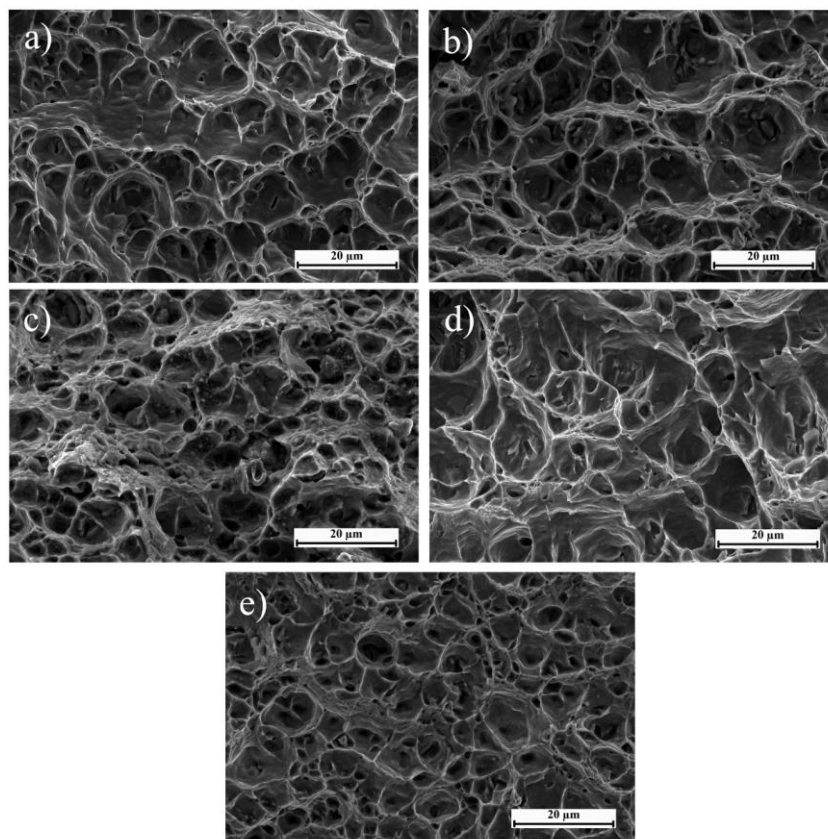


Figure 7. SEM fractographs of the samples a) T0, b)  $190 \text{ }^\circ\text{C}$ -2 h, c)  $190 \text{ }^\circ\text{C}$ -4 h, d)  $205 \text{ }^\circ\text{C}$ -2 h and e)  $205 \text{ }^\circ\text{C}$ -4 h.

#### 4. Conclusions

This study investigated the effects of post-weld heat treatment on the microstructural and mechanical properties of age-hardenable Al-Zn-Mg-Si-Cu aluminium alloy plates welded by friction stir welding (FSW) method. The main results obtained are as follows:

- No failure was detected in the weld zone after FSW, but significant onion ring formation was observed, especially in artificially aged specimens.
- As a result of grain refinement in the weld zone with FSW, hardening with grain boundary strengthening occurred.
- AlFeSi precipitates were detected in the artificially aged specimens, which showed an increase in microhardness over the entire welded section, including the friction stir zone, due to Orowan hardening.
- These specimens reached a peak aging parameter of 190 °C and 4 hours of soaking time, and the ultimate tensile strength was 210.8 N·mm<sup>-2</sup>.
- Ductile fracture mode was observed in all annealed and artificially aged specimens.

#### Declaration

The authors declared no potential conflicts of interest with respect to the research, authorship, and/or publication of this article. The author) also declared that this article is original, was prepared in accordance with international publication and research ethics, and ethical committee permission or any special permission is not required.

#### Author Contributions

D.Arslan and S.I.Ayvaz developed the methodology together. D.Arslan and S.I.Ayvaz performed the analysis together. S.I. Ayvaz supervised and improved the study. D.Arslan and S.I.Ayvaz wrote the manuscript together.

#### References

1. Ayvaz, S. I., D. Arslan, and M. Ayvaz, *Investigation of mechanical and tribological behaviour of SiC and B<sub>4</sub>C reinforced Al-Zn-Mg-Si-Cu alloy matrix surface composites fabricated via friction stir processing*. Materials Today Communications, 2022. **31**(103419). <https://doi.org/10.1016/j.mtcomm.2022.103419>.
2. Ayvaz, M., *Determination of the effect of artificial aging parameters on dry sliding wear resistance of 6013 aluminum alloy (Al-Mg-Si-Cu)*. International Advanced Researches and Engineering Journal, 2021. **05**(02): p. 181-187. <https://doi.org/10.35860/iarej.839108>.
3. Cetinel, H. and M. Ayvaz, *The Effect of Aging Parameters and Roughness on the Wear Properties of Aluminum Alloy 6082*. Materials Testing, 2014. **56**(11-12): p. 988-993.
4. Ma, Z. Y., S.R. Sharma, and R.S. Mishra, *Microstructural modification of as-cast Al-Si-Mg alloy by friction stir processing*. Metallurgical and Materials Transactions A, 2006. **37**(11): p. 3323-3336.
5. Georgantzia, E., M. Gkantou, and G.S. Kamaris, (2021) *Aluminium alloys as structural material: A review of research*. Engineering Structures, 2021. **227**: 111372
6. Bolat, Ç., B. Ergene, U. Karakılıç, and a. Gökşenli, *Investigating on the machinability assessment of precision machining pumice reinforced AA7075 syntactic foam*. Proceedings of the Institution of Mechanical Engineers, Part C: Journal of Mechanical Engineering Science, 2021. **236**(5): p. 1-15. <https://doi.org/10.1177/09544062211027613>.
7. WANHILL, R.J.H., *Aerospace applications of aluminum-lithium alloys*. In: *Aluminum-lithium Alloys*. Butterworth-Heinemann, 2014. p. 503-535.
8. Cheng, Y., Y. Hu, J. Xu, L. Yu, T. Huang, and H. Zhang, *Studies on microstructure and properties of TiB<sub>2</sub>-Al<sub>3</sub>Ti ceramic particles reinforced spray-formed 7055 aluminum alloy fusion welded joints*. Journal of Materials Research and Technology, 2022. **19**(13): p. 1298-1311. <https://doi.org/10.1016/j.jmrt.2022.05.116>.
9. Murali, N., Y. Chi, and X. Li, *Natural aging of dissimilar high-strength AA2024/AA7075 joints arc welded with nano-treated filler*. Materials Letters, 2022. **322**: 132479. <https://doi.org/10.1016/j.matlet.2022.132479>.
10. Hu, Z., S. Yuan, X. Wang, G. Liu, and Y. Huang, *Effect of post-weld heat treatment on the microstructure and plastic deformation behavior of friction stir welded 2024*. Materials and Design, 2011. **32**(10): p. 5055-5060. <https://doi.org/10.1016/j.matdes.2011.05.035>.
11. Lin, S., J. Tang, S. Liu, Y. Deng, H. Lin, H. Ji, L. Ye, and X. Zhang, *Effect of travel speed on microstructure and mechanical properties of fsw joints for Al-Zn-Mg alloy*. Materials, 2019. **12**: 4178. <https://doi.org/10.3390/ma12244178>.
12. Aydin, H., A. Bayram, and I. Durgun, *The effect of post-weld heat treatment on the mechanical properties of 2024-T4 friction stir-welded joints*, Materials and Design, 2010. **31**: p. 2568-2577. <https://doi.org/10.1016/j.matdes.2009.11.030>.
13. Yeni, C., S. Sayer, O. Ertugrul, and M. Pakdil, *Effect of post-weld aging on the mechanical and microstructural properties of friction stir welded aluminum alloy 7075*. Archives of Materials Science and Engineering, 2008. **34**(2): p. 105-109.
14. Cabibbo, M., A. Forcelllese, E. Santecchia, C. Paoletti, S. Spigarelli, and M. Simoncini, *New Approaches to Friction Stir Welding of Aluminum Light-Alloys*. Metals, 2020. **10**(2): 233. <https://doi.org/10.3390/met10020233>.
15. Su, J., T.W. Nelson, and C.J. Sterling, *Microstructure evolution during FSW/FSP of high strength aluminum alloys*. Materials Science and Engineering A, 2005. **405**(1-2): p. 277-286. <https://doi.org/10.1016/j.msea.2005.06.009>.
16. Awang Draup, A.J., B. Rodgers, P.B. Prangnell, Q.M. Li, M.J. Lunt, and J.D. Robson, *Modelling of friction stir welded AA2139 aluminium alloy panels in tension and blast*. International Journal of Impact Engineering, 2022. **163**: p. 104163. <https://doi.org/10.1016/j.ijimpeng.2022.104163>.
17. Rhodes, C.G., M.W. Mahoney, W.H. Bingel, R.A.

- Spurling, and C.C. Bampton, *Effects of friction stir welding on microstructure of 7075 aluminum*. Scripta Materialia, 1997. **36**(1): p. 69–75.
18. Su, J., T.W. Nelson, and C.J. Sterling, *Microstructure evolution during FSW/FSP of high strength aluminum alloys*. Materials Science and Engineering A, 2005. **405**(1-2): p. 277-286. [https://doi.org/10.1016/S1359-6454\(02\)00449-4](https://doi.org/10.1016/S1359-6454(02)00449-4).
  19. Chen, Y.C., J.C. Feng, and H.J. Liu, *Precipitate evolution in friction stir welding of 2219-T6 aluminum alloys*. Materials Characterization, 2009. **60**(6): p. 476–481. <https://doi.org/10.1016/j.matchar.2008.12.002>.
  20. Rajendran, C., K. Srinivasan, V. Balasubramanian, H. Balaji, and P. Selvaraj, *Influences of post weld heat treatment on tensile strength and microstructure characteristics of friction stir welded butt joints of AA2014-T6 aluminum alloy*. Journal of the Mechanical Behavior of Materials, 2016. **25**(3–4): p.89–98. <https://doi.org/10.1515/jmbm-2016-0011>.
  21. Yadav, V.K., V. Gaur, and I.V. Singh, *Effect of post-weld heat treatment on mechanical properties and fatigue crack growth rate in welded AA-2024*. Materials Science and Engineering: A, 2020. **779**: 139116. <https://doi.org/10.1016/j.msea.2020.139116>.
  22. Elangovan, K. and V. Balasubramanian, *Influences of post-weld heat treatment on tensile properties of friction stir-welded AA6061 aluminum alloy joints*. Materials Characterization, 2008. **59**: p. 1168–1177. <https://doi.org/10.1016/j.matchar.2007.09.006>.
  23. Ipekoglu, G., S. Erim, and G. Cam, *Investigation into the influence of post-weld heat treatment on the friction stir welded AA6061 Al-Alloy plates with different temper conditions*. Metallurgical and Materials Transactions A: Physical Metallurgy and Materials Science, 2014. **45**(2): p. 864–877. <https://doi.org/10.1007/s11661-013-2026-y>.
  24. Sharma, C., D.K. Dwivedi, and P. Kumar, *Effect of post weld heat treatments on microstructure and mechanical properties of friction stir welded joints of Al-Zn-Mg alloy AA7039*. Materials and Design, 2013. **43**: p. 134–143. <https://doi.org/10.1016/j.matdes.2012.06.018>.
  25. Al-Allaq, A.H., M. Ojha, Y.S. Mohammed, S.N. Bhukya, Z. Wu, and A.A. Elmustafa, (2023). *Post-weld heat treatment effects on microstructure, crystal structure, and mechanical properties of donor stir-assisted friction stir welding material of AA6061-T6 alloy*. The International Journal of Advanced Manufacturing Technology, 2023. **129**: p. 1845-1854.
  26. Zhang, C., G. Huang, D. Zhang, Z. Sun, and Q. Liu, *Microstructure and mechanical properties in dissimilar friction stir welded AA2024/7075 joints at high heat input: effect of post-weld heat treatment*. Journal of Materials Research and Technology, 2020. **9**(6): p. 14771-14782. <https://doi.org/10.1016/j.jmrt.2020.10.053>.
  27. Masoumi Khalilabad, M., Y. Zedan, D. Texier, M. Jahazi, and P. Bocher, *Effect of heat treatments on microstructural and mechanical characteristics of dissimilar friction stir welded 2198/2024 aluminum alloys*. Journal of Adhesion Science and Technology, 2021. **36**(3): p. 221–239.
  28. Maji, P., R.K. Nath, R. Karmakar, P. Paul, R.K.B. Meitei, S.K. Ghosh, *Effect of post processing heat treatment on friction stir welded/processed aluminum based alloys and composites*. CIRP Journal of Manufacturing Science and Technology, 2021. **35**: p. 96-105. <https://doi.org/10.1016/j.cirpj.2021.05.014>
  29. Abu-Okail, M., I. Sabry, a. Abu-Okail and W.M. Shewakh, *Effect of Changing Heat treatment conditions on microstructural and mechanical properties of friction stir welded sheets of AA2024 with Interlayer Strip Width AA7075*. Journal of Failure Analysis and Prevention, 2020. **3**: p. 701-722
  30. Feng, J.C., Y.C. Chen, and H. J. Liu, *Effects of post-weld heat treatment on microstructure and mechanical properties of friction stir welded joints of 2219-O aluminium alloy*. Materials Science and Technology, 2006. **22**(1): p. 86–90. <https://doi.org/10.1179/174328406X79298>.
  31. Sree Sabari, S., V. Balasubramanian, S. Malarvizhi, and G. Madusudhan Reddy, *Influences of post weld heat treatment on tensile properties of friction stir welded AA2519-T87 aluminium alloy joints*. Journal of the Mechanical Behavior of Materials, 2021. **24**(5–6): p. 195–205. <https://doi.org/10.1515/jmbm-2015-0021>.
  32. Pabandi, H.K., H.R. Jasnani, and M. Paidar, *Effect of precipitation hardening heat treatment on mechanical and microstructure features of dissimilar friction stir welded AA2024-T6 and AA6061-T6 alloys*. Journal of Manufacturing Processes, 2018. **31**: p. 214–220.
  33. Zhao, Y.H., S.B. Lin, L. Wu, and F. X. Qu, *The influence of pin geometry on bonding and mechanical properties in friction stir weld 2014 Al alloy*. Materials Letters, 2005. **59**(23): p. 2948–2952. <https://doi.org/10.1016/j.matlet.2005.04.048>.
  34. Chen, Y., H. Liu, and J. Feng, *Friction stir welding characteristics of different heat-treated-state 2219 aluminum alloy plates*. Materials Science and Engineering: A, 2006. **420**(1–2): p. 21–25. <https://doi.org/10.1016/j.msea.2006.01.029>.
  35. Radisavljevic, I., A. Zivkovic, N. Radovic, and V. Grabulov, *Influence of FSW parameters on formation quality and mechanical properties of Al 2024-T351 butt welded joints*. Transactions of Nonferrous Metals Society of China (English Edition), 2013. **23**(12): p. 3525–3539. [https://doi.org/10.1016/S1003-6326\(13\)62897-6](https://doi.org/10.1016/S1003-6326(13)62897-6).
  36. Kwon, Y.J., S.B. Shim, and D.H. Park, *Friction stir welding of 5052 aluminum alloy plates*. Transactions of Nonferrous Metals Society of China (English Edition), 2009. **19**(1): p. 23-27. [https://doi.org/10.1016/S1003-6326\(10\)60239-7](https://doi.org/10.1016/S1003-6326(10)60239-7).
  37. Kalemba, I., S. Dymek, C. Hamilton, and M. Blicharski, *Microstructure evolution in friction stir welded aluminium alloys*. Archives of Metallurgy and Materials, 2009. **54**(1): p. 75-82.
  38. Krishnan, K.N., *On the formation of onion rings in friction stir welds*. Materials Science and Engineering: A, 2002. **327**(2): p. 246-251.
  39. Wang, Z., L. Huang, J. Li, X. Li, H. Zhu, F. Ma, H. Ma, and Cui, J., *Microstructure and properties of friction stir welded 2219 aluminum alloy under heat treatment and electromagnetic forming process*. Metals, 2018. **8**(5): p. 305-316. <https://doi.org/10.3390/met8050305>.
  40. Sutton, M.A., B. Yang, A.P. Reynolds, and R. Taylor,

- Microstructural studies of friction stir welds in 2024-T3 aluminum.* Materials Science and Engineering: A, 2002. **323**(1-2): p. 160-166.
41. Aydın, H., *Quality and properties of the friction stir welded AA2024-T4 aluminium alloy at different welding conditions.* Materials Testing, 2010. **52**(9): p. 640-650. <https://doi.org/10.3139/120.110172>.
  42. Sajadifar, S.V., G. Moeini, E. Scharifi, C. Lauhoff, S. Böhm, and T. Niendorf, *On the Effect of Quenching on Postweld Heat Treatment of Friction-Stir-Welded Aluminum 7075 Alloy.* Journal of Materials Engineering and Performance, **28**(8): p. 5255-5265.
  43. Sato Y.S., Hç. Kokawa, M. Enomoto, S. Jogan. and T. Hashimoto, *Precipitation Sequence in Friction Stir Weld of 6063 Aluminum during Aging.* Metallurgical and Materials Transactions A, 1999. **30**: p. 3125-3130.
  44. Aydın, H., O. Tuncel, C. Yuce, M. Tutar, N. Yavuz, and A. Bayram, *Effect of rotational speed and dwell time on mechanical properties of dissimilar AA1050-AA3105 friction stir spot welded joints.* Materials Testing, 2014. **56**(10): p. 818-825. <https://doi.org/10.3139/120.110636>.
  45. Sedmak, A., M.M.M., Eramah, S. Tadić, S. Perković, and H. Dascau, *Impact Toughness of Friction Stir Welded Al-Mg Alloy.* Materials Testing, 2014. **56**(10): p. 837-841. <https://doi.org/10.3139/120.110638>.
  46. Ojo, O.O., E. Taban, and E. Kaluc, *Effect of residual Alclad on friction stir spot welds of AA2219 alloys.* Materials Testing, 2018. **60**: p. 979-988. <https://doi.org/10.3139/120.111245>.
  47. Sato, Y.S., M. Urata, H. Kokawa, and K. Ikeda, *Hall-Petch relationship in friction stir welds of equal channel angular-pressed aluminium alloys.* Materials Science and Engineering: A, 2003. **354**(1-2): p. 298-305. [https://doi.org/10.1016/S0921-5093\(03\)00008-X](https://doi.org/10.1016/S0921-5093(03)00008-X).
  48. Saldaña-Garcés, R., D. Hernández-García, F. García-Vázquez, E.J. Gutiérrez-Castañeda, D. Verderra, and R. Deaquino-Lara, *Friction stir welding of dissimilar AA6061-T6 to AZ31B-H24 alloys.* Soldagem & Inspeção, 2020. **25**: p. 1-14. <https://doi.org/10.1590/0104-9224/SI25.25>.
  49. Tao, X., Chang, Y., Guo, Y., Li, W., and Li, M., *Microstructure and mechanical properties of friction stir welded oxide dispersion strengthened AA6063 aluminum matrix composites enhanced by post-weld heat treatment.* Materials Science and Engineering: A, 2018. **725**: p. 19-27. <https://doi.org/10.1016/j.msea.2018.03.094>.
  50. Saravanan, V., Rajakumar, S., and Muruganandam, A., *Effect of friction stir welding process parameters on microstructure and mechanical properties of dissimilar AA6061-T6 and AA7075-T6 aluminum alloy joints.* metallography, Microstructure, and Analysis, 2016. **5**(6): p. 476-485. <https://doi.org/10.1007/s13632-016-0315-8>.
  51. Sivaraj, P., D. Kanagarajan, and V. Balasubramanian, *Effect of post-weld heat treatment on mechanical properties and fatigue crack growth behaviour of friction stir welded 7075-T651 Al alloy.* Transactions of Nonferrous Metals Society of China, 2014. **24**(8): p. 2459-2467.
  52. Bayazid, S.M., H. Farhangi, H. Asgharzadeh, L. Radan, A. Ghahramani, and A. Mirhaji, *Effect of cyclic solution treatment on microstructure and mechanical properties of friction stir welded 7075 Al alloy.* Materials Science and Engineering: A, 2016. **649**: p. 293-300.
  53. Kumar, P.V., G.M., Redd, and K.S. Rao, *Microstructure, mechanical and corrosion behavior of high strength AA7075 aluminium alloy friction stir welds e Effect of post weld heat treatment.* Defence Technology, 2015. **11**(2): p. 166-173.
  54. İpekoğlu, G. and G. Çam, *Effects of initial temper condition and postweld heat treatment on the properties of dissimilar friction-stir-welded joints between AA7075 and aAA6061 aluminum alloys.* Metallurgical and Materials Transactions A, 2014. **45**(7): p.3074-3087.
  55. Lakshminarayanan, A. K., V. Balasubramanian, and K. Elangovan, *Effect of welding processes on tensile properties of AA6061 aluminium alloy joints.* International Journal of Advanced Manufacturing Technology, 2009. **40**(3-4): p. 286-296. <https://doi.org/10.1007/s00170-007-1325-0>.